Received: 21 April 2022 | Revised: 26 June 2022 | Accepted: 8 July 2022

DOI: 10.1002/prot.26399

RESEARCH ARTICLE

PROTEINS WILEY

Analysis of amyloidogenic transthyretin mutations using continuum solvent free energy calculations

Julian Hartmann | **Martin Zacharias**

Physics Department and Center of Protein Assemblies, Technical University of Munich, Garching, Bavaria, Germany

Correspondence
Martin Zacharias, Physics Department and Center of Protein Assemblies, Technical University of Munich, Garching, Bavaria 85748, Germany.
Email: martin.zacharias@ph.tum.de

Funding information
Deutsche Forschungsgemeinschaft

Abstract

Many proteins can undergo pathological conformational changes that result in the formation of amyloidogenic fibril structures. Various neurodegenerative diseases are associated with such pathological fibril formation of specific proteins. Transthyretin (TTR) is a tetrameric globular transport protein in the blood plasma that can dissociate, unfold, and form long and stable fibrils. Many TTR mutations are known that promote (TTR) amyloidosis and cause severe diseases. TTR amyloidosis has been studied extensively using biochemical methods and structures of various mutations in the globular form have been characterized. Recently, also the structure of a TTR fibril has been determined. In an effort to better understand why some mutations increase or decrease the tendency of amyloid formation, we have applied a combined molecular dynamics and continuum solvent approach to calculate the energetic influence of residue changes in the globular versus fibril form. For 29 out of 36 tested TTR single residue mutations, the approach correctly predicts the increased or decreased tendency for amyloidosis allowing us also to elucidate the origins of the tendency. We find that indeed the destabilization of the globular monomer or changes in dimer and tetramer stability due to mutation has a dominant influence on the amyloidogenic tendency. The continuum solvent model predicts a significantly more favorable mean energy per residue of the fibril form compared to the globular form. This effect is only slightly modulated by single-point mutations preserving the energetic preference for fibril formation upon protein unfolding. It explains why no correlation between experimental amyloidosis and calculated change in fibril stability was observed.

KEYWORDS
amyloid fibrils, amyloid stability, fibril formation, MMGBSA calculation, pathological fibril disease, single-point mutation

1 | INTRODUCTION

Transthyretin (TTR) is a transport protein for thyroid hormone thyroxine (T_4) and retinol binding protein.[1] It is produced mainly in the liver, but also (<5%) in the choroid plexus of the brain and the retinal pigment epithelium.[2]

TTR forms a symmetric tetramer, consisting of four identical monomers. Each monomer is characterized by a large predominance of β-strands. The tetramer is formed by the association of two dimers that are in equilibrium with the monomeric proteins.[3–6] Andrade[7] and Falls et al.[8] first described the occurrence of amyloidosis of TTR in 1952 and 1955, respectively, which means the pathological formation

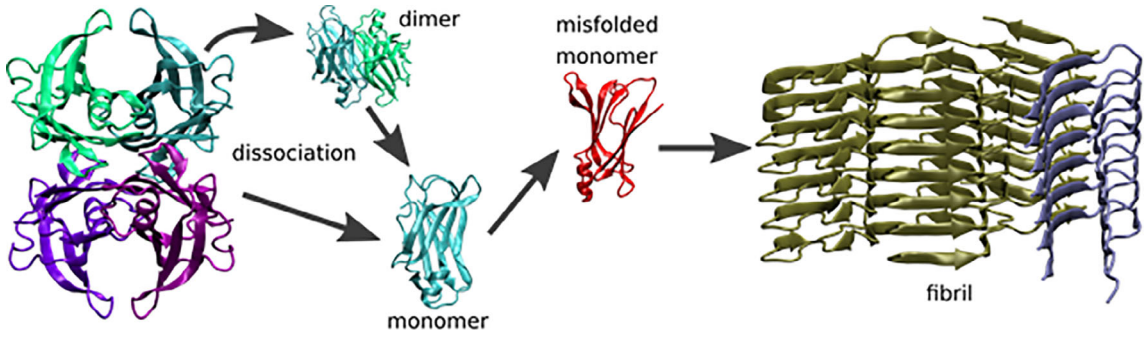

FIGURE 1 Schematic pathway to TTR amyloid fibril formation. For amyloidosis, the native TTR tetramer structure (cartoon representation with different colors for each monomer) dissociates into dimers and finally monomers, which then unfold (or at least partially unfold). The unfolded monomers align to each other forming a fibril structure where each layer arises from one monomer. Note that the structures of some residues are not resolved in the CryoEM fibril structure, leading to two fragments per layer (visualized by two different colors).

of long and stable fibrils consisting of misfolded parallel aligned TTR molecules.[9] Amyloidosis can also be caused by many other proteins resulting in severe diseases like Alzheimer's disease or Parkinson's disease.[10] Today three different types of TTR amyloidosis (ATTR) are known, which all result in severe diseases.[2,11–13] The wild-type (WT) form of ATTR is also called senile systemic amyloidosis (SSA) since it normally affects elderly people. The fibrils deposit mainly in the heart causing stiffness and thickening of the muscle. Autopsies of supercentenarians exposed SSA being responsible for 70% of their deaths.[8] The other two disease forms, familial amyloid cardiomyopathy and familial amyloid polyneuropathy, are hereditary since they are caused by gene mutations of the TTR gene resulting in disease causing point mutations of the protein.[14–16] Similar to SSA the heart and kidneys are affected, but in contrast to SSA, these diseases manifest much earlier within the affected person's span of life.

In order to form amyloid aggregates, the TTR tetramer has to dissociate to the monomeric form that unfolds and can form aggregates (see Figure 1). Hence, both mutations that increase the intrinsic propensity for β-aggregation or stabilize the amyloid plaque structure but also mutations that destabilize the TTR tetramer or folded monomer may cause increased ATTR. Indeed, more than 100 mutations are known that affect ATTR.[15,17] However, there are also known mutations that prevent amyloid production by enhancing the stability of the tetramer, monomer, or reduce the β-aggregation tendency. An improved understanding of the mechanism of how mutations affect ATTR could be helpful for further development of therapeutic drug treatments.[18] Until recently, the only therapy was the transplantation of heart and/or liver in affected patients. Today there are several promising treatment approaches. Some aim at reducing protein production of harmful TTR-variants by blocking RNA-translation with short interfering RNA sequences binding specifically to the corresponding mRNA in TTR-producing cells or using antisense oligonucleotides.[19,20] Other drug molecules bind to TTR and stabilize its natural tetrameric structure.[21–25] A promising binding site for these drugs seems to be the binding pocket for thyroxine (e.g., for Tafamidis[21,22] or Diflunisal[23,24]), which, however, also reduces the ability to transport thyroxine. A third route explores the possibility to remove harmful fibrils with monoclonal antibodies that bind to misfolded monomers, fibrils, or prefibrillar TTR and induce phagocytic clearance by macrophages.[26–29]

Experimental crystal structures of the number of TTR variants in the folded tetrameric form have been determined.[4–6,30–32] These structural studies indicate small variations in loop regions or local segments around the mutation site but no major conformational changes that may directly explain a reduced tendency of unfolding or tetramer formation. However, for some TTR mutations, a reduced tetramer association compared to wild type has been found using biophysical techniques.[33] Combined experimental and molecular simulation approaches on the globular TTR indicate that indeed the tetramer stability and the unfolding tendency of the TTR monomer are of key importance for the tendency of a TTR mutant to form amyloids.[5,17,25] However, these studies so far did not include the TTR amyloid structure. Recently, a CryoEM structure of the TTR amyloid has been determined.[34] Together with the crystal structures of the globular tetrameric form, this allows one to study the effect of mutations on the stability of the globular form, the unfolded form, and the amyloid form using free energy simulations. In principle, among the most accurate methods are alchemical free energy simulations to transform amino acid side chains in the different TTR forms and to record associated free energy changes. However, such techniques are computationally quite demanding and often allow to study only few mutations.[17] Our aim is to employ a less demanding end-point free energy method to investigate systematically a large set of TTR mutations. The method is based on running short Molecular Dynamics (MD) simulations of the WT and the mutated proteins in the different conformational states and evaluate the generated trajectories using a continuum solvent model (MMGBSA: Molecular Mechanics Generalized Born Surface Area method).[35,36] To avoid large conformational changes during the simulation's weak positional restraints on the structures were included, assuming that the mutations do not alter the structure significantly compared to wild type. Indeed, crystal structures of TTR mutations indicate only small conformational changes in the globular form compared to wild type.[5,30,31] The approach was applied to 36 TTR mutations for which either an increased (A25T,[37] V30G,[38]

V30M,[5,39,40] D38A,[12] S52P,[41,42] E54G,[15,43] E54K,[43] L55P,[44,45] L58H,[46] T60A,[16,47] E61K,[48] S77Y,[49] Y78F,[50] I84A,[51] I84S,[40] H88S,[52] H88R,[52] E89K,[53] Y114C,[54–57] Y114H,[25] V122I[58]) or decreased (S85P,[3] H88A,[52] H88F,[52] H88Y,[52] E92P,[40] V94P,[3] R104H,[5] A108I,[59] A108V,[59] A108W,[59] A109V,[59] A109T,[60] T119M,[61] T119W,[3] and T119Y[3]) tendency for amyloidosis has been reported experimentally. Since experimentally only a tendency for amyloidosis is known it allowed us only a qualitative comparison with calculated stability changes. For 29 out of 36 mutations, our calculations agreed qualitatively with the experimental tendency and could be used to identify the origins of this tendency. The simulations indicate that mutations can both stabilize or destabilize the globular tetrameric form but also the amyloid structure to various degrees. Overall, the tendency of mutations to promote increased or decreased amyloidosis correlates strongly with the destabilization of the globular or dimeric/tetrameric forms but much less or not with the calculated destabilization/stabilization of the amyloid structure. Similar results were also obtained using alternative methods to evaluate protein stability such as FoldX.[62] The influence of neighboring residues and structural and energetic origins of the tendencies are discussed. The rapid methodology can also be used to systematically analyze mutation effects in other amyloid forming systems assuming that the structural changes are small.

2 | MATERIALS AND METHODS

As starting structure for the globular TTR protein the protein database entry pdb6e6z[3] was used. It represents the tetrameric structure. The coordinates of the Tafamidis drug molecule were removed (not included in the simulations). The specific structure was selected because of best overlap in sequence with the given fibril structure (less unresolved residues compared to other pdb-entries). The mutations were created by replacing the corresponding side chains and adjustment of side chain structures by selecting the sterically best fitting rotamer and energy minimization. The structure of the amyloid fibril form corresponds to the entry pdb6sdz.[34] The mutations of the fibril were created in the same way as for the globular protein. A fibril was represented by seven protein chains to minimize the effect of the protein water boundary at both ends of the oligomeric fibril.

Employing the Amber18 software[63] package solvated starting structures were generated, using the ff14SB force field[64] for proteins and the OPC water model.[65] The globular protein structures were embedded in octahedral water boxes with a minimum distance of 10.0 Å between the protein and the box boundary. For the fibrils, cubic boxes were found to be optimal with respect to overall system size. Sodium and chloride ions were added to neutralize the charge of the systems and to obtain a ~100 mM salt concentration. After a minimization run of 500 steps (250 steepest descent algorithm and 250 conjugate gradient algorithm) the systems were heated up linearly to 300 K within 200 ps followed by 50 ps equilibration with constant volume periodic boundary conditions and restraints on all heavy atoms (2.1 kcal mol^{-1} $Å^{-2}$). Subsequently, the systems were relaxed for 100 ps at constant pressure (1.0 bar) and the positional restraints were reduced in four steps of 0.5 kcal mol^{-1} $Å^{-2}$. Each time the system was simulated for 50 ps with the final state of the previous simulation taken as reference for the positional restraints, allowing the mutated structures to adjust. This leads to conformationally relaxed backbone structures to accommodate the mutated side chain. At a final restraint level of 0.1 kcal mol^{-1} $Å^{-2}$, the system relaxed for 3 ns before the data gathering run of 2 ns was performed. For all simulations, a time step of 2 fs and a 10.0 Å real space cutoff was chosen (the PME method was used to account for long-range electrostatic interactions). All bonds involving hydrogens were constrained by SHAKE.[66] The SETTLE algorithm was used to constraint bond length in water molecules.[67] Data gathering simulations were performed at a constant pressure of 1 bar and temperature of 300 K using a Langevin thermostat.

The end-point free energy calculations were performed using the MMGBSA tools of the Amber18 package. The explicit water molecules and ions were removed from the trajectories and the sampled conformations were re-evaluated using a Generalized Born continuum model using the mbondi3 radii and parameters from the study by Nguyen et al.[68] (igb = 8 in Amber) in combination with a surface area-dependent tension model to account for nonpolar solvation (surface tension coefficient $\gamma = 0.005$ kcal mol^{-1} $Å^{-2}$) was used. Between 100 and 10 000 trajectory frames were used to obtain mean energy contributions. No conformational entropy changes were considered; hence, we assume that the change in mobility due to mutation is similar in the globular versus fibril form. For representing the energy change associated with a mutation in an unfolded protein the central residue of a tripeptide in an extended conformation was considered (includes at nearest neighbor effects in the unfolded chain upon residue mutations).

For comparison, all mutations were also analyzed using the FoldX modeling program suite.[63] Within the BuildModel tool FoldX employs an internal structural optimization upon mutagenesis and evaluates single conformations of structures using a knowledge-based combination of energy terms. The effect of a mutation is obtained as score relative to the wild-type sequence. It was applied to all mutations in globular and fibril form.

3 | RESULTS

3.1 | Influence of mutations on fibril and tetramer stability

The formation of TTR amyloid structures requires the dissociation of the TTR tetramer, unfolding of the monomer and formation of the amyloid arrangement (Figure 1). Hence, a mutation can influence the free energy change associated with each step. The application of the MMGBSA method[35] is a relatively fast computational approach that allows us to investigate the contribution of each conformational transition on a large set of TTR mutations (for comparison, we also used the even faster FoldX method[62]). Calculations were performed for the

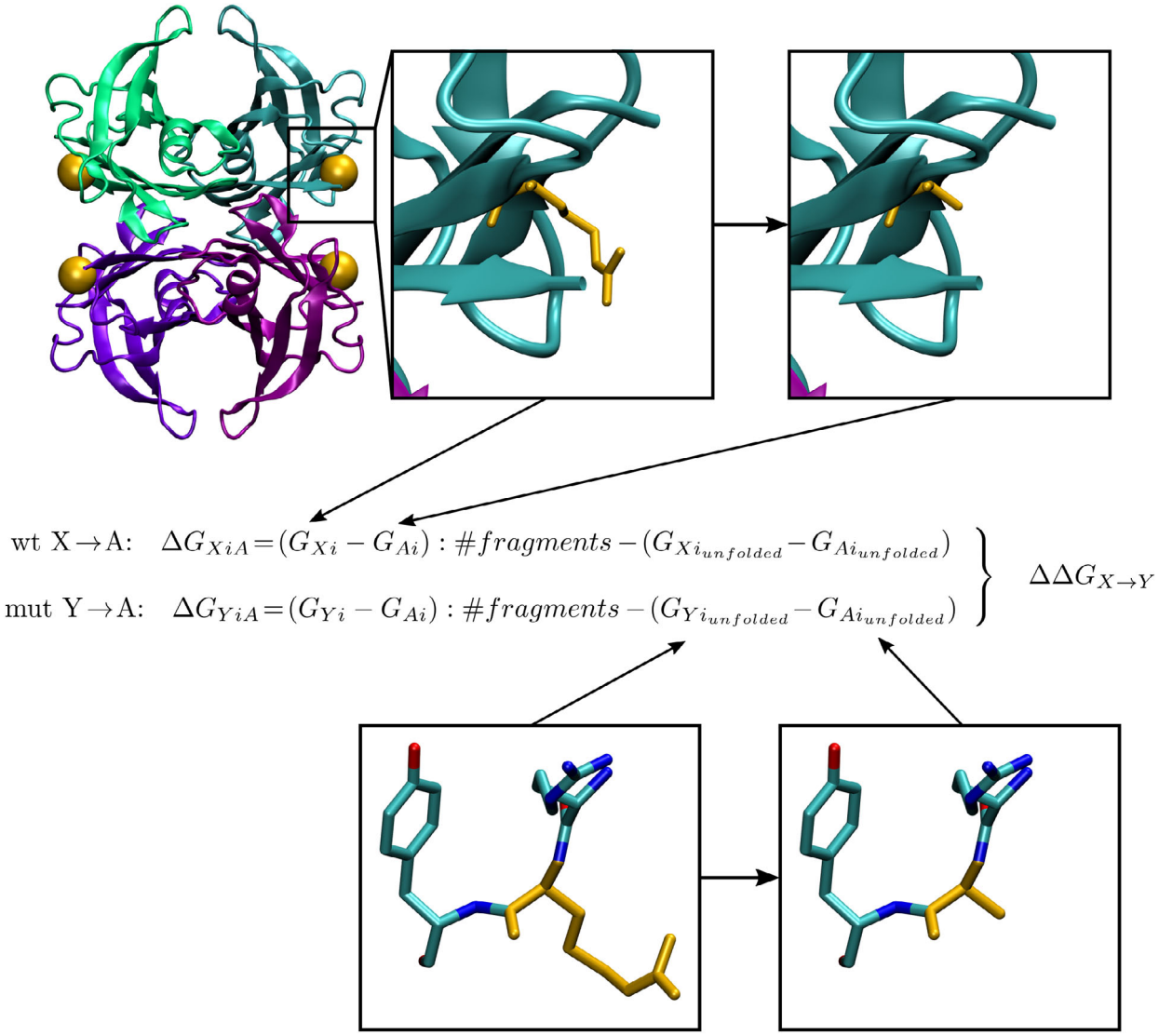

FIGURE 2 Schematic illustration of the MMPBSA calculations of single residue substitutions (marked yellow, in the tetramer the position is indicated as yellow sphere). To obtain mean energy differences of single-point mutations, first the energy contribution of a specific residue is calculated by cutting all atoms after the C_β-atom of this residue (Ala-scan) and subtracting the mean energy of the unfolded sequence by calculating the energy of the specific residue and its next neighbors. This is done for the wild type and the mutated protein resulting in the free energy contribution difference of the single residue/side chain.

mutations in the fibril structure and the monomer, dimer and tetramer structures (illustrated in Figure 2). The computer time (on a single core) for running the simulations of the globular and amyloid forms of each TTR mutation and MMGBSA evaluation takes ~2–3 h computer time (using 500 trajectory frames for MMGBSA analysis, however, for the cases investigated here we analyzed in each case 10 000 frames). For the present study, we investigated 36 TTR variants for which experimental data on the amyloid forming tendency are available (location of the mutations is presented in Figure 3).

In order to directly compare the calculations to the amyloid forming tendency we consider first the difference of the mean energy contribution of the selected side chain mutation for forming the tetramer structure versus forming the fibril structure (Figure 4). The energies are calculated with respect to the unfolded solvated side chain (represented as central residue in a solvated tripeptide).

Each mutant was initially created based on the same tetrameric template structure (pdb6e6z,[3] see Section 2) or the same fibril structure (pdb6sdz). Hence, we assume that both the globular and the fibril structure are similar for all mutations and do not cause major conformational changes or formation of a new fibril structure. Also, experimental (quantitative) data on how a mutation changes the amyloid fibril stability is not available, only an amyloidosis tendency for forming fibrils of each TTR variant can be obtained experimentally. Hence, one can distinguish mutations that increase (red background in Figure 4) or decrease (yellow background in Figure 4) the tendency for amyloid fibril formation. For most, that is 29 of the 36 cases, our

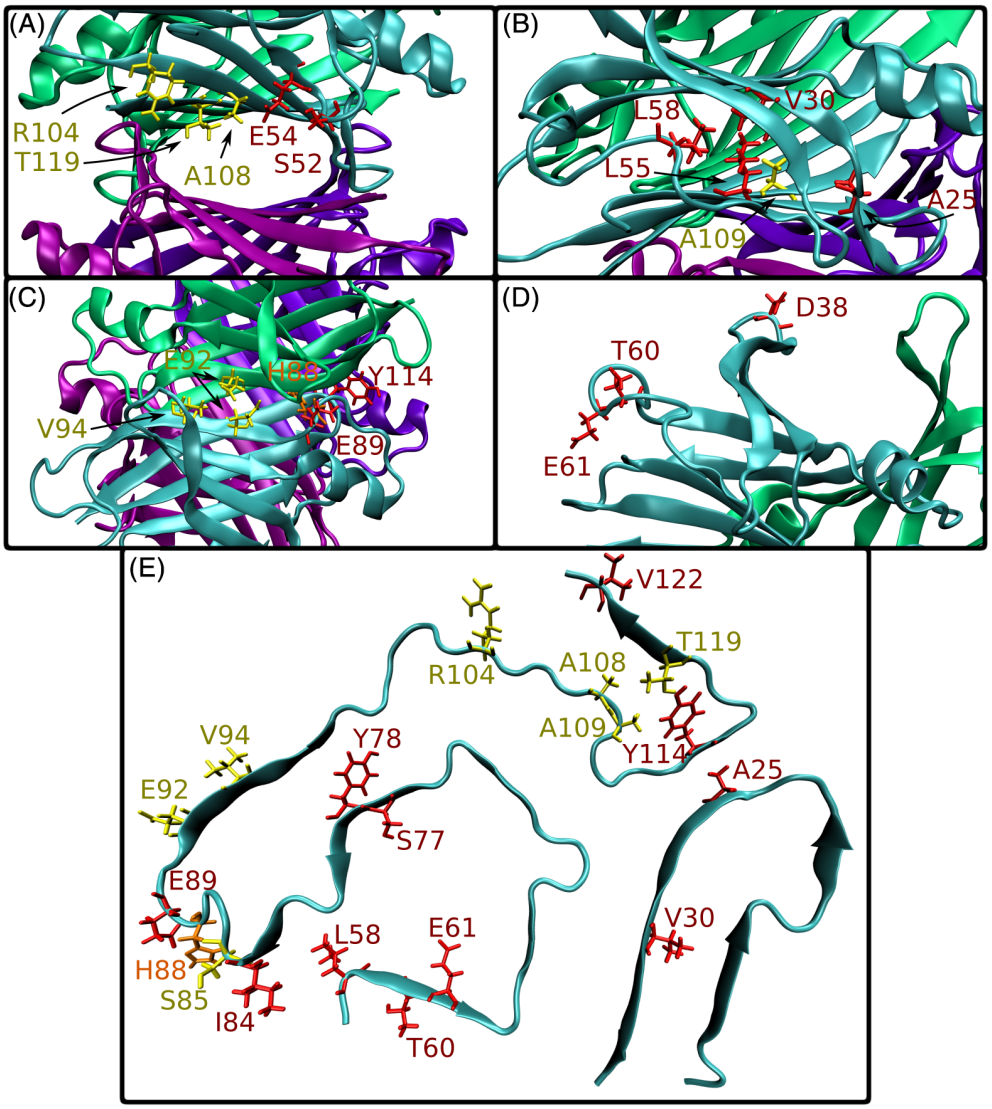

FIGURE 3 Location of mutations within the globular tetramer (A–D, pdb6e6z) and fibril (E, pdb6sdz). Relevant sidechains (of the wild type) are shown as sticks with red colored residues representing mutation positions that were found to increase amyloidosis tendency (yellow: opposite behavior). Within the tetramer mutation positions can be oriented towards the cavity between the two dimers (shown in A), the buried region between the monomer's β-sheets (B), the interface between the monomers within each dimer (C, both at the interface and in the rim region around the interface) or are solvent exposed in the globular tetramer (D, also exposed in the dimer and monomer). Mutation positions are also mapped on the known fibril structure (E, pdb6sdz, only one layer is shown for clarity).

calculations correctly reproduce the experimentally obtained fibril formation tendency (Figure 4).

Interestingly, for most known amyloidogenic mutations (V30G,[38] D38A,[12] E54G,[15,43] E54K,[43] L55P,[44] L58H,[46] T60A,[16] E61K,[48] S77Y,[49] Y78F,[50] I84A,[51] I84S,[40] H88S,[52] H88R,[52] Y114C,[54] and Y114H[25]) our results indicate a significant overall destabilizing effect on the tetramer. Note, that at this analysis stage influences on monomer stability, dimer formation and energetics of dimer association to tetramers are all included (decomposition see next paragraph). Interestingly, the calculations predict that the fibril structure is sometimes even slightly or considerably destabilized or less stabilized for most of these variants compared to the wild type.

Among the known nonamyloidogenic mutations, the calculations yield for most cases including S85P,[3] H88F,[52] H88Y,[52] V94P,[3] A108I,[59] A108V,[59] A108W,[3] A109V,[60] A109T,[60] T119M,[61] T119W[3] and T119Y[3] an energetically stabilizing effect on the tetramer compared to wild type. Surprisingly, several of the nonamyloidogenic mutations are predicted to stabilize also the amyloid form albeit to a lesser degree than the stabilization of the tetramer (Figure 4, yellow part). In several of the nonamyloidogenic cases, however, no or only very small effects on the fibril stability relative to wild type were found. Overall, the results indicate a rather strong correlation between calculated stabilizing/destabilizing effect of a mutation on tetramer formation and experimentally observed tendency for fibril formation. In contrast, no good correlation was found between known amyloid forming tendency of the mutations and relative energetic stabilization of the fibril structure (only for the V30M, the E61K, and the S77Y a significant stabilization of the fibril form is predicted that outscores the effect on the globular form).

In addition to MMGBSA calculations, we also employed the FoldX approach[62] to predict the effect of mutations on the stability of globular versus fibril conformation of TTR. The BuildModel option in FoldX allows conformational optimization upon mutation and energetic evaluation based on a knowledge-based optimal combination of energy terms (on single conformations). Interestingly, very similar to the MMGBSA analysis, it also predicts for almost all amyloidogenic mutation cases a destabilization of the globular form and for most nonamyloidogenic cases a stabilization of the globular tetrameric form

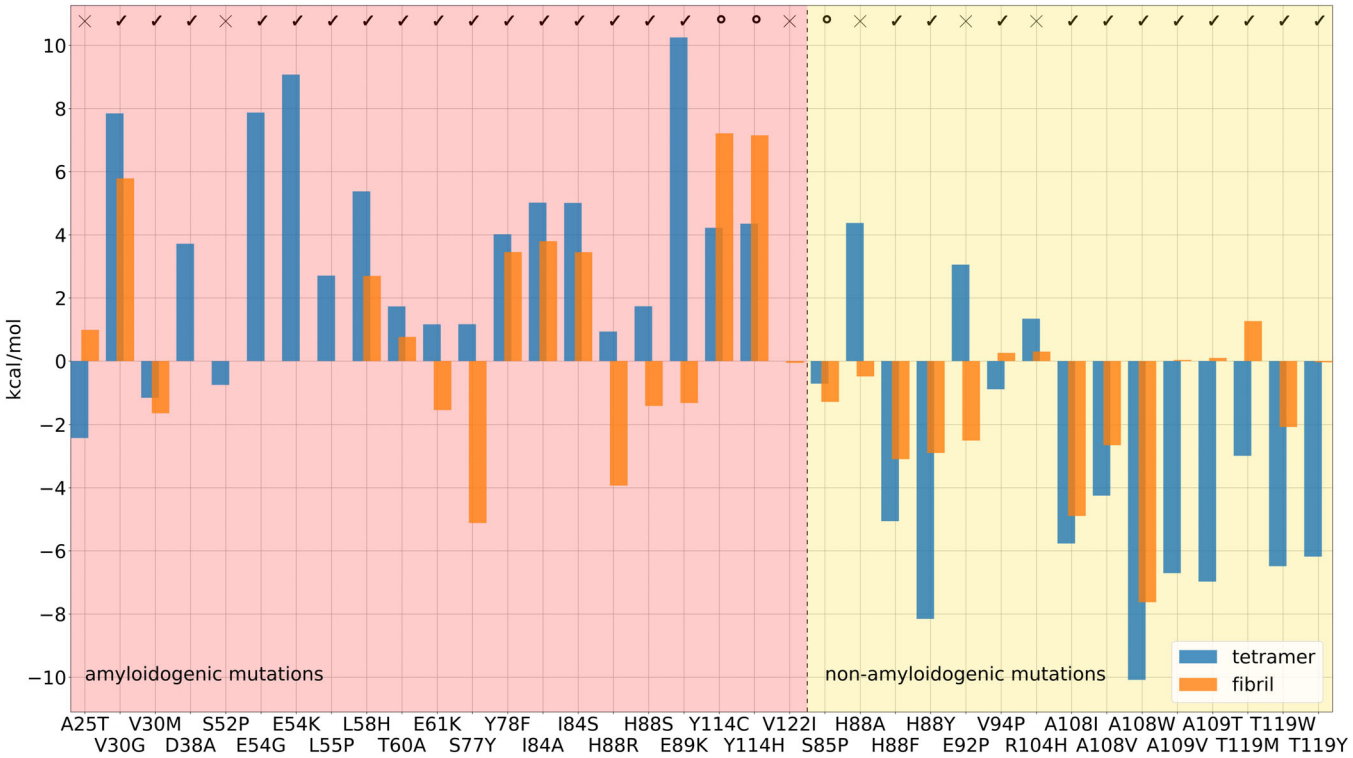

FIGURE 4 Energy contribution (boxes) of single-point mutations of Transthyretin in tetrameric (blue) and fibril (orange) form. The mutations are indicated on the *x*-axis. A negative/positive contribution implies a stabilization/destabilization of the structure. All energies are per monomer/layer; however, all fragments/layers were included in the calculations and the result was divided by number of chains (4 or 7 for the tetramer or the fibril, respectively). Since the sequence of the fibril includes a gap compared to the tetramer, there are no fibril energy values for some variants (D38A, S52P, E54G, E54K, and L55P). A red background indicates that this mutation is known for its increased amyloidogenicity, whereas a yellow background means that the mutant reduces amyloidosis or stabilizes the tetrameric form. The symbols at the top depict if the result matches to experimental data (check mark) or partially matches (circle) or does not match (cross).

(Figure S1). FoldX predicts for most mutations a small destabilizing effect on the TTR fibril structure and for several of the nonamyloidogenic mutations an extremely strong fibril destabilization (10–20 kcal mol^{-1} per mutated residue). These predictions possibly overestimate the destabilization since FoldX has been designed and trained for the application on globular protein structures. Nevertheless, the predictions by FoldX show qualitatively the same trend and confirm the results obtained with the MMGBSA approach.

Since the calculated stability changes of mutations in the fibril form showed only little or no correlation with the experimentally observed ATTR tendency we calculated the mean (absolute) MMGBSA energy per residue for the globular (tetramer) form and for the fibril form. It turned out that the MMGBSA energy is ~2 kcal mol^{-1} more negative per residue than the globular form. This result varies for the mutations but is overall similar to wild type (Figure S2). It indicates that according to the MMGBSA calculations, the fibril structure (embedded in the fibril) is energetically much more stable than the globular form. This in turn implies that the small change due to mutation of a single residue may not change the large favorisation of the fibril form. Hence, once the globular form is unfolded at sufficiently high concentration the fibril form is in all cases energetically strongly favored. However, the energetic favorisation of

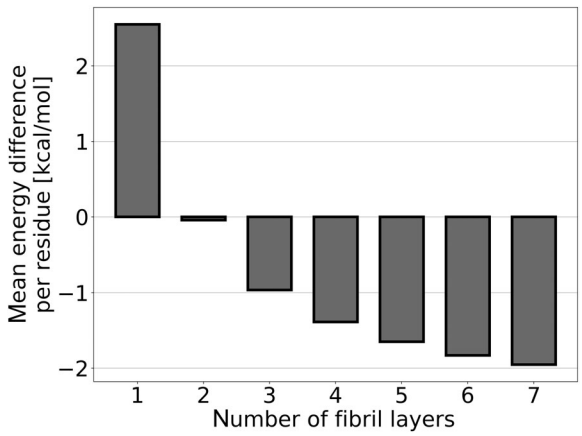

FIGURE 5 Calculated mean MMGBSA energy difference per residue between tetrameric globular TTR and TTR in the fibril structure versus number of layers in the fibril

the fibril form depends on the number of peptide layers included in the MMGBSA evaluation (Figure 5). Considering just one chain in the fibril conformation results in a mean energy per residue in favor of the globular form. In this case, the fibril backbone of the protein is fully solvent exposed without forming hydrogen bonds to a neighboring

layer. However, already three layers forming a fibril results in a calculated mean energy per residue in favor of the fibril eventually reaching a level of ~ -2 kcal mol^{-1} per residue (Figure 5).

For some mutations, the MMGBSA calculations do not agree with the experimental trend of ATTR. For example, for the variant A25T, the calculations predict a decreased stability of the fibril and increased stability of the tetramer although experimentally this mutation causes increased ATTR. Visual inspection shows that the A25 is located at a narrow-buried interface between two β-strand segments in the fibril structure (Figure 3). Indeed, replacement by a larger polar threonine can perturb this interface. It is possible that such variant forms an altered fibril topology with an increased space in the fibril not considered in the present study. It is also possible that some mutations promote fibril formation by stabilizing intermediates during amyloid formation. Such mutation can change the kinetics of fibril formation without stabilizing the final fibril structure. The possibility of an altered fibril structure could also explain the results for mutations Y114C and Y114H. The mutations to smaller residues destabilize the globular form but more strongly also the fibril structure. An altered fibril topology or adjustments of the fibril structure not considered in the present study may reduce the predicted destabilization effect on the fibril. Also, the H88R variant,[52] known to promote amyloidosis, is predicted to destabilize the globular tetramer and also to stabilize the fibril structure. In this case, the protonation states of the wild-type histidine (we assume the standard neutral protonation state) may influence the calculated stabilities. Experimental studies have shown, that at neutral pH His88 is neutrally protonated, but at lower pH values changes to double protonation state, which destabilizes the WT structure.[69]

Indeed, the H88A,[52] E92P[40] (artificial) and R104H[5] variants are known to reduce amyloidosis but the calculations predict a destabilization of the tetramer possibly due to changes in protonation states not considered in the present calculations. For example, in the case of the V30M variant,[5,34,40] the calculations indicate a slight stabilization of the tetramer and a stronger stabilization of the fibril. In this case, a rather small calculated effect is expected because both methionine and valine are hydrophobic side chains of not very different size. A similar explanation may hold for mutation V122I[34,70] for which the calculations predicted no change in amyloidogenic tendency. Indeed, the variant V30G corresponding to the loss of a whole nonpolar sidechain shows a strong effect that agreed qualitatively with the experiment. The result of the amyloidogenic variant S52P[41,42] also does not fit to experimental data. This could be due to changes in the backbone structure that may affect the fibril topology due to replacement by proline. However, in this case, other known in vivo influences (not considered by our calculations) like an enhanced proteolytic cleavage between Lys48 and Thr49, favored by this mutation, may drive the formation of fibrils.[71]

The MMGBSA analysis allows us also to separate the effect of a mutation into energetic contributions to both for the globular tetramer and the fibril structure (Figures S3–S6). For the bonded energy contributions, destabilizing and stabilizing effects are observed with no clear correlation with the amyloidogenic effect of the mutations (Figure S3). Also, no clear distinction between amyloidogenic and non-amyloidogenic variants is observed for electrostatic and van der Waals contributions except that both contributions show a significant anticorrelation (Figures S4 and S5). The surface area dependent nonpolar solvation term (Figure S6) correlates strongly with the van der Waals contribution. This is expected since the reduction of surface area often also leads to stronger packing energies. Interestingly, if a mutation leads to decreased or increased van der Waals interaction this is typically seen then for both the globular and the fibril TTR form.

3.2 | Influence of mutations on tetramer, dimer, and monomer formation

Depending on the position of a mutation, its impact may affect the folding stability of a single monomer, formation of a dimer or formation of the tetrameric complex formed by two dimers (Figures 1 and 6). As reference state for the calculations, the transition in the unfolded structure (represented as central residue in a tripeptide) was used. The calculated relative stability changes for the tetramer are the same as given in Figure 4 and the stability change is given per monomer unit. Thus, in the plots of Figure 6, identical values for monomer, dimer, and tetramer indicate that the mutation changes only the folding of the monomer but has no further influence on the dimer and tetramer association. This concerns most of the investigated mutations (see Figure 4). However, some mutations, especially of residue 88 and 89 and 114 show a modest change in monomer stability but a significant change in relative free energy of dimer formation (no or only slight further stability change upon tetramer formation). Among the mutations that promote amyloid formation there are five cases (E54K, I84A, I84S, Y114C, and Y114H) for which a destabilization of the tetramer is observed and vice versa there are also six cases among the mutations that reduce the ATTR (A108I, A108V, A108W, T119M, T119W, and T119Y) with a predicted increase in tetramer stability. Indeed, residues 108, 119 are located at the dimer–dimer interface (Figure 3) and large residues can fill empty space at the interface. In some of the latter cases, the stabilization of the globular forms is also due to increases folding stability. Overall, the calculations indicate that stabilization or destabilization of each step up to the tetrameric globular form can influence the ATTR tendency. The effects on dimer and tetramer formation can be correlated to the location of the residues at or close to an interface between the monomers in the dimer (H88, Y114, E92, and V94) or the interface between dimers in the tetramer (A108, T119, see Figure 3).

3.3 | Optimizing the efficiency of the calculations

In the above MMGBSA calculations, we analyzed for each mutation case 10 000 frames of each simulation. This resulted in calculated errors of the mean well below 1.0 kcal mol^{-1} for the calculations of the whole tetramer as well as the fibril. However, the MMGBSA calculations on these many frames exceeds (considerably) the simulation time for generating the trajectory frames. Predictions based on FoldX that took ~24 h for all 36 mutations are faster mainly because no MD

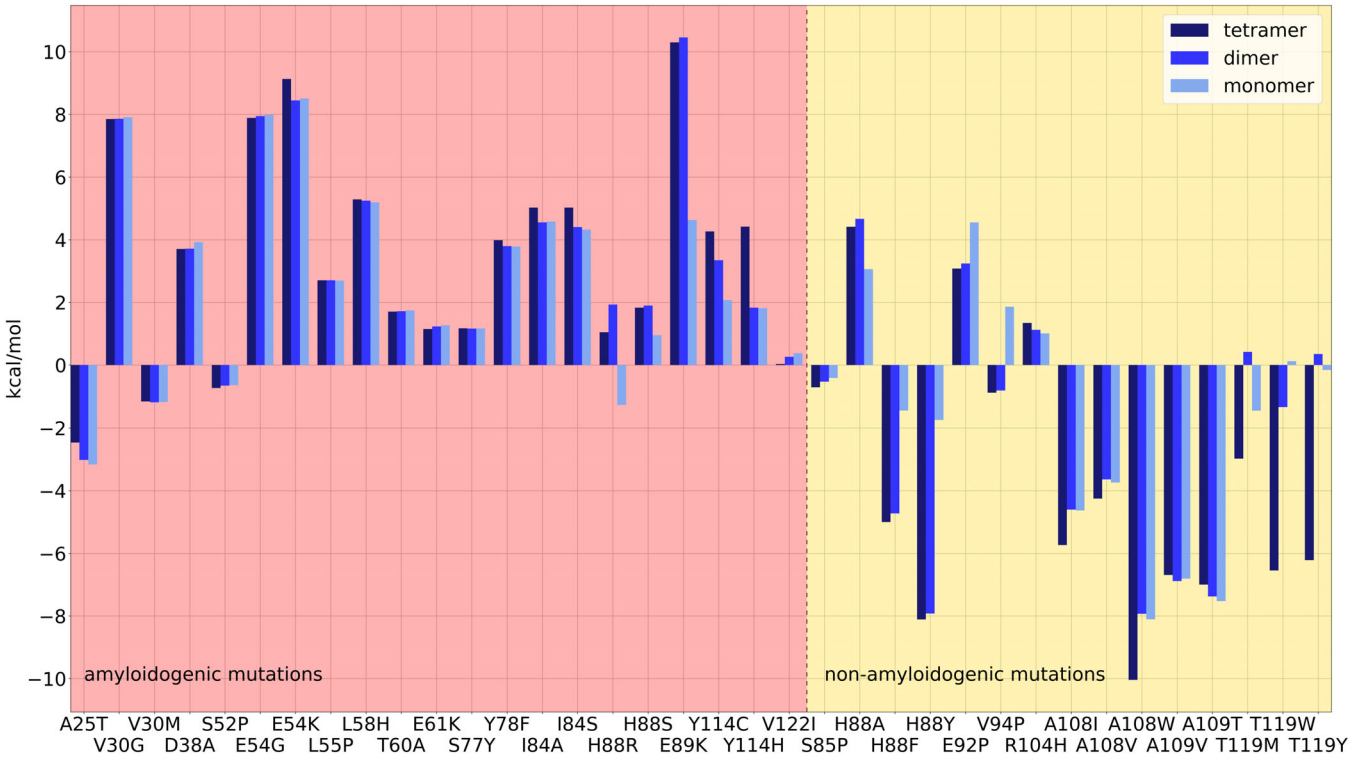

FIGURE 6 Comparison of calculated energy changes for tetramers, dimers and monomers upon mutation (relative to wild type). The mutations are indicated on the *x*-axis. A negative/positive contribution implies a stabilization/destabilization of the structure. All energies are per monomer/layer.

simulation to generate an ensemble of conformations is required and gave qualitatively similar results (except for some mutations in the fibril structure that resulted in very high penalties).

An ensemble of structures allows one to estimate an error of the calculated energies. In order to speed up the overall calculations and balance each part, we systematically reduced the number of frames used for the MMGBSA approach down to only 10 (distributed equally over the whole simulation). Interestingly, despite an increase in calculated error of the mean (>10 kcal mol^{-1} in some cases for the evaluation of only 10 frames) the mean calculated energy values changed only very little (Figure S7). The error per selected residue (seven copies in case of seven fibril layers) is also lower than for the whole molecule and allows one to speed up the MMGBSA calculation. Hence, it indicates that for a rapid estimation of mutation effects, the evaluation of just a few hundred frames might be sufficient and the generation and evaluation (including simulation and MMGBSA calculation) is then a matter of minutes for each mutation. Also note that the evaluation of each mutation can be performed independently in parallel which further speeds up the evaluation of mutation effects.

4 | DISCUSSION

A significant number of human proteins can undergo amyloidosis resulting in unfolding and formation of amyloidogenic fibrils that cause various degenerative diseases.[2,15,71] Recently, the structures of both the globular forms and the amyloid fibril forms of several of these proteins have been determined. Especially, the rapidly growing number of fibril structures also formed under different in vivo or ex vivo conditions become available due progress in the structure determination by CryoEM techniques. However, there is still very little understanding why certain protein sequences possess a strong tendency for fibril formation, why certain mutations increase or decrease the tendency of fibril formation and which structural form (folded, unfolded, or fibril) has the largest influence.[72] Simulation studies can be helpful to obtain insight into the molecular details and also energetics of fibril formation and the influence of mutations. However, available methods to quantify relative stability changes are often time consuming especially in case of systematic applications. A second goal of the present study was also to evaluate the possibility of using an MMGBSA (or even simpler FoldX) approach to rapidly estimate mean energy changes due to mutations applied to the TTR system for which experimental data on many mutations are available. For ~80% of the 36 tested mutations, the calculations predicted a tendency in correct agreement with the experiment. The failure in a few cases can be due to changes in the protonation states of charged residues but may also be due to possible changes in the fibril structure due to a mutation. These effects are not accounted for in the present protocol. However, one should also keep in mind that only a qualitative comparison to experiment is possible because experimentally only the qualitative increase or decrease of ATTR tendency is available.

The calculations allowed us also to extract some important conclusions concerning the influence of the mutations on the ATTR. The systematic application to 36 TTR mutations indicates that it is indeed the destabilization of the globular forms that strongly correlates with ATTR tendency in agreement with previous studies based on studying limited sets of mutations.[5,16] Similar results were obtained for application of FoldX. The effect, however, cannot be attributed to one of the possible sub-equilibria such as monomer folding, dimer formation, or tetramer formation but can be caused by influencing either one or several of these steps. The analysis of energetic contributions of each mutation also did not identify a single energy term responsible for modulating the tendency of fibril formation of a given mutation.

Interestingly, mutations that are predicted to increase or decrease the fibril stability relative to wild type are approximately equally distributed among those that either show enhanced or reduced amyloidogenic tendencies. It indicates that according to the calculations once the TTR is monomeric and (partially) unfolds a reduced stability of the fibril (relative to wild type) has only little influence of ATTR (the residual stability of the fibril is still sufficient to drive fibril formation). Calculations on the mean energy per residue in the globular versus fibril form indicate indeed a significant energetic stabilization of the amyloid fibril form compared to the globular structure offering a direct explanation for the above conclusion. Interestingly, the energetic favorisation of the fibril is predicted to depend significantly on the number of layers included in the calculations. Formation of an initial single layer is energetically strongly unfavored compared to the globular form but already a fibril composed of just three layers has a mean MMGBSA energy per residue that favors the fibril structure.

Finally, we demonstrated that the approach is rapid enough for the systematic application on large numbers of mutations for a given globular and fibril protein structure. It was found that approaches such as FoldX are also useful to evaluate the tendency but since the method is based on an empirically optimized weighting of different energy terms (for globular proteins) it might be useful to extend this also to studies on amyloid fibril structures. It has been shown recently that some peptide or protein sequences can adopt several different fibril topologies depending on the sequence and experimental conditions for amyloid fibril formation.[73] In cases where such alternative fibril topologies are available, it is also possible to evaluate the preference of a mutation to promote the formation of different fibrils.

AUTHOR CONTRIBUTIONS

Julian Hartmann: Data curation; Formal analysis; Visualization; Writing – original draft; Methodology; Investigation; Software. **Martin Zacharias**: Conceptualization; Writing – original draft; Methodology; Investigation; Supervision; Project administration; Writing – review and editing; Validation; Funding acquisition; Resources.

ACKNOWLEDGMENTS

The authors thank S. Chen and Dr. M. Hitzenberger and for helpful discussions. This work was supported by the Deutsche Forschungsgemeinschaft SFB1035 (Project number 2013022640, project B02). Open Access funding enabled and organized by Projekt DEAL.

PEER REVIEW

The peer review history for this article is available at https://publons.com/publon/10.1002/prot.26399.

DATA AVAILABILITY STATEMENT

The data that support the findings of this study are available from the corresponding author upon reasonable request.

ORCID

Martin Zacharias https://orcid.org/0000-0001-5163-2663

REFERENCES

1. Benson MD, Uemichi T. Transthyretin amyloidosis. *Amyloid*. 1996;3:44-56.
2. Gertz MA, Benson MD, Dyck PJ, et al. Diagnosis, prognosis, and therapy of transthyretin amyloidosis. *J Am Coll Cardiol*. 2015;66:2451-2466.
3. Saelices L, Johnson LM, Liang WY, et al. Uncovering the mechanism of aggregation of human transthyretin. *J Biol Chem*. 2015;290:28932-28943.
4. Schormann N, Murrell JR, Benson MD. Tertiary structures of amyloidogenic and non-amyloidogenic transthyretin variants: new model for amyloid fibril formation. *Amyloid*. 1998;5:175-187.
5. Cendron L, Trovato A, Seno F, et al. Amyloidogenic potential of transthyretin variants: insights from structural and computational analyses. *J Biol Chem*. 2009;284:25832-25841.
6. Hamilton JA, Steinrauf LK, Braden BC, et al. The x-ray crystal structure refinements of normal human transthyretin and the amyloidogenic Val-30-->Met variant to 1.7-A resolution. *J Biol Chem*. 1993;268:2416-2424.
7. Andrade C. A peculiar form of peripheral neuropathy: familiar atypical generalized amyloidosis with special involvement of the peripheral nerves. *Brain*. 1952;75:408-427.
8. Falls HF, Jackson JJ, Carey JH, Rukivina JG, Block WD. Ocular manifestations of hereditary primary systemic amyloidosis. *AMA Arch Ophthalmol*. 1955;54:660-664.
9. Jacobson DR, Pastore RD, Yaghoubian R, et al. Variant-sequence transthyretin (Isoleucine 122) in late-onset cardiac amyloidosis in black Americans. *N Engl J Med*. 1997;336:466-473.
10. Nguyen PH, Ramamoorthy A, Sahoo BR, et al. Amyloid oligomers: a joint experimental/computational perspective on Alzheimer's disease, Parkinson's disease, type II diabetes, and amyotrophic lateral sclerosis. *Chem Rev*. 2021;121:2545-2647.
11. Westermark P, Sletten K, Johansson B, Cornwell GG. Fibril in senile systemic amyloidosis is derived from normal transthyretin. *Proc Natl Acad Sci U S A*. 1990;87:2843-2845.
12. Cho HJ, Yoon JY, Bae MH, et al. Familial transthyretin amyloidosis with variant Asp38Ala presenting with orthostatic hypotension and chronic diarrhea. *J Cardiovasc Ultrasound*. 2012;20:209-212.
13. Planté-Bordeneuve V, Said G. Familial amyloid polyneuropathy. *Lancet Neurol*. 2011;10:1086-1097.
14. Coles LS, Young RD. Supercentenarians and transthyretin amyloidosis: the next frontier of human life extension. *Prev Med*. 2012;54:S9-S11.
15. Reilly MM, Adams D, Booth DR, et al. Transthyretin gene analysis in European patients with suspected familial amyloid polyneuropathy. *Brain*. 1995;118:849-856.
16. Gillmore JD, Damy T, Fontana M, et al. A new staging system for cardiac transthyretin amyloidosis. *Eur Heart J*. 2018;39:2799-2806.
17. Yee AW, Aldeghi M, Blakeley MP, et al. A molecular mechanism for transthyretin amyloidogenesis. *Nat Commun*. 2019;10:925.

18. Müller ML, Butler J, Heidecker B. Emerging therapies in transthyretin amyloidosis—a new wave of hope after years of stagnancy? *Eur J Heart Fail*. 2020;22:39-53.
19. Bennett CF. Therapeutic antisense oligonucleotides are coming of age. *Annu Rev Med*. 2019;70:307-321.
20. Niemietz CJ, Sauer V, Stella J, et al. Evaluation of therapeutic oligonucleotides for familial amyloid polyneuropathy in patient-derived hepatocyte-like cells. *PLOS One*. 2016;11:e0161455.
21. Coelho T, Maia LF, Martins da Silva A, et al. Tafamidis for transthyretin familial amyloid polyneuropathy: a randomized, controlled trial. *Neurology*. 2012;79:785-792.
22. Merlini G, Planté-Bordeneuve V, Judge DP, et al. Effects of tafamidis on transthyretin stabilization and clinical outcomes in patients with non-Val30Met transthyretin amyloidosis. *J Cardiovasc Transl Res*. 2013;6:1011-1020.
23. Berk JL, Suhr OB, Obici L, et al. Repurposing diflunisal for familial amyloid polyneuropathy: a randomized clinical trial. *JAMA*. 2013;310:2658-2667.
24. Sekijima Y, Dendle MA, Kelly JW. Orally administered diflunisal stabilizes transthyretin against dissociation required for amyloidogenesis. *Amyloid*. 2006;13:236-249.
25. Sekijima Y, Campos RI, Hammarström P, et al. Pathological, biochemical, and biophysical characteristics of the transthyretin variant Y114H (p.Y134H) explain its very mild clinical phenotype. *J Peripher Nerv Syst*. 2015;20:372-379.
26. Bodin K, Ellmerich S, Kahan MC, et al. Antibodies to human serum amyloid P component eliminate visceral amyloid deposits. *Nature*. 2010;468:93-97.
27. Su Y, Jono H, Torikai M, et al. Antibody therapy for familial amyloidotic polyneuropathy. *Amyloid*. 2012;19(Suppl 1):45-46.
28. Phay M, Blinder V, Macy S, et al. Transthyretin aggregate-specific antibodies recognize cryptic epitopes on patient-derived amyloid fibrils. *Rejuvenation Res*. 2014;17:97-104.
29. Planque SA, Nishiyama Y, Hara M, et al. Physiological IgM class catalytic antibodies selective for transthyretin amyloid. *J Biol Chem*. 2014;289:13243-13258.
30. Damas AM, Ribeiro S, Lamzin VS, Palha JA, Saraiva MJ. Structure of the Val122Ile variant transthyretin—a cardiomyopathic mutant. *Acta Crystallogr D Biol Crystallogr*. 1996;52:966-972.
31. Zanotti G, Folli C, Cendron L, et al. Structural and mutational analyses of protein-protein interactions between transthyretin and retinol-binding protein. *FEBS J*. 2008;275:5841-5854.
32. Hamilton JA, Steinrauf LK, Braden BC, Murrell JR, Benson MD. Structural changes in transthyretin produced by the Ile 84 Ser mutation which result in decreased affinity for retinol-binding protein. *Amyloid*. 1996;3:1-12.
33. Jenne DE, Denzel K, Blätzinger P, et al. A new isoleucine substitution of Val-20 in transthyretin tetramers selectively impairs dimer-dimer contacts and causes systemic amyloidosis. *Proc Natl Acad Sci U S A*. 1996;93:6302-6307.
34. Schmidt M, Wiese S, Adak V, et al. Cryo-EM structure of a transthyretin-derived amyloid fibril from a patient with hereditary ATTR amyloidosis. *Nat Commun*. 2019;10:5008.
35. Wang C, Greene D, Xiao L, Qi R, Luo R. Recent developments and applications of the MMPBSA method. *Front Mol Biosci*. 2018;4:87.
36. Siebenmorgen T, Zacharias M. Computational prediction of protein–protein binding affinities. *WIREs Comput Mol Sci*. 2020;10:e1448.
37. Azevedo EPC, Pereira HM, Garratt RC, Kelly JW, Foguel D, Palhano FL. Dissecting the structure, thermodynamic stability, and aggregation properties of the A25T Transthyretin (A25T-TTR) variant involved in leptomeningeal amyloidosis: identifying protein partners that co-aggregate during A25T-TTR fibrillogenesis in cerebrospinal fluid. *Biochemistry*. 2011;50:11070-11083.
38. Petersen RB, Goren H, Cohen M, et al. Transthyretin amyloidosis: a new mutation associated with dementia. *Ann Neurol*. 1997;41:307-313.
39. Holmgren G, Hellman U, Lundgren H-E, Sandgren O, Suhr OB. Impact of homozygosity for an amyloidogenic transthyretin mutation on phenotype and long term outcome. *J Med Genet*. 2005;42:953-956.
40. Zanotti G, Cendron L, Folli C, Florio P, Imbimbo BP, Berni R. Structural evidence for native state stabilization of a conformationally labile amyloidogenic transthyretin variant by fibrillogenesis inhibitors. *FEBS Lett*. 2013;587:2325-2331.
41. Mangione PP, Porcari R, Gillmore JD, et al. Proteolytic cleavage of Ser52Pro variant transthyretin triggers its amyloid fibrillogenesis. *Proc Natl Acad Sci U S A*. 2014;111:1539-1544.
42. Stangou AJ, Hawkins PN, Heaton ND, et al. Progressive cardiac amyloidosis following liver transplantation for familial amyloid polyneuropathy: implications for amyloid fibrillogenesis. *Transplantation*. 1998;66:229-233.
43. Miyata M, Sato T, Mizuguchi M, et al. Role of the glutamic acid 54 residue in transthyretin stability and thyroxine binding. *Biochemistry*. 2010;49:114-123.
44. Jacobson DR, McFarlin DE, Kane I, Buxbaum JN. Transthyretin Pro55, a variant associated with early-onset, aggressive, diffuse amyloidosis with cardiac and neurologic involvement. *Hum Genet*. 1992;89:353-356.
45. Castro-Rodrigues AF, Gales L, Saraiva MJ, Damas AM. Structural insights into a zinc-dependent pathway leading to Leu55Pro transthyretin amyloid fibrils. *Acta Crystallogr D Biol Crystallogr*. 2011;67:1035-1044.
46. Nichols WC, Liepnieks JJ, McKusick VA, Benson MD. Direct sequencing of the gene for Maryland/German familial amyloidotic polyneuropathy type II and genotyping by allele-specific enzymatic amplification. *Genomics*. 1989;5:535-540.
47. Wallace MR, Dwulet FE, Conneally PM, Benson MD. Biochemical and molecular genetic characterization of a new variant prealbumin associated with hereditary amyloidosis. *J Clin Invest*. 1986;78:6-12.
48. Murakami T, Yokoyama T, Mizuguchi M, et al. A low amyloidogenic E61K transthyretin mutation may cause familial amyloid polyneuropathy. *J Neurochem*. 2021;156:957-966.
49. Wallace MR, Dwulet FE, Williams EC, Conneally PM, Benson MD. Identification of a new hereditary amyloidosis prealbumin variant, Tyr-77, and detection of the gene by DNA analysis. *J Clin Invest*. 1988;81:189-193.
50. Terazaki H, Ando Y, Fernandes R, Yamamura K, Maeda S, Saraiva MJ. Immunization in familial amyloidotic polyneuropathy: counteracting deposition by immunization with a Y78F TTR mutant. *Lab Invest*. 2006;86:23-31.
51. Pasquato N, Berni R, Folli C, Alfieri B, Cendron L, Zanotti G. Acidic pH-induced conformational changes in amyloidogenic mutant transthyretin. *J Mol Biol*. 2007;366:711-719.
52. Yokoyama T, Hanawa Y, Obita T, Mizuguchi M. Stability and crystal structures of His88 mutant human transthyretins. *FEBS Lett*. 2017;591:1862-1871.
53. Nakamura M, Asl KH, Benson MD. A novel variant of transthyretin (Glu89Lys) associated with familial amyloidotic polyneuropathy. *Amyloid*. 2000;7:46-50.
54. Ueno S, Uemichi T, Yorifuji S, Tarui S. A novel variant of transthyretin (Tyr114 to Cys) deduced from the nucleotide sequences of gene fragments from familial amyloidotic polyneuropathy in Japanese sibling cases. *Biochem Biophys Res Commun*. 1990;169:143-147.
55. Ueno S, Fujimura H, Yorifuji S, et al. Familial amyloid polyneuropathy associated with the transthyretin Cys114 gene in a Japanese kindred. *Brain J Neurol*. 1992;115(Pt 5):1275-1289.

56. Haagsma E, Post J, DeJager A, Nikkels P, Hamel B, Hazenberg B. A Dutch kindred with familial amyloidotic polyneuropathy associated with the transthyretin Cys 114 mutant. *Amyloid*. 1997;4:112-117.
57. Eneqvist T, Olofsson A, Ando Y, et al. Disulfide-bond formation in the transthyretin mutant Y114C prevents amyloid fibril formation in vivo and in vitro. *Biochemistry*. 2002;41:13143-13151.
58. Gorevic PD, Prelli FC, Wright J, Pras M, Frangione B. Systemic senile amyloidosis. Identification of a new prealbumin (transthyretin) variant in cardiac tissue: immunologic and biochemical similarity to one form of familial amyloidotic polyneuropathy. *J Clin Invest*. 1989;83:836-843.
59. Sant'Anna R, Almeida MR, Varejão N, et al. Cavity filling mutations at the thyroxine-binding site dramatically increase transthyretin stability and prevent its aggregation. *Sci Rep*. 2017;7:44709.
60. Steinrauf LK, Hamilton JA, Braden BC, Murrell JR, Benson MD. X-ray crystal structure of the Ala-109-->Thr variant of human transthyretin which produces euthyroid hyperthyroxinemia. *J Biol Chem*. 1993;268(4):2425-2430.
61. Saraiva MJ, Almeida MR, Alves IL, et al. Modulating conformational factors in transthyretin amyloid. *Ciba Found Symp*. 1996;199:47-52. discussion 52–57.
62. Schymkowitz J, Borg J, Stricher F, Nys R, Rousseau F, Serrano L. The FoldX web server: an online force field. *Nucleic Acids Res*. 2005;33:W382-W388.
63. Case DA, Ben-Shalom IY, Brozell SR, et al. *AMBER 18*. University of California; 2018.
64. Maier JA, Martinez C, Kasavajhala K, Wickstrom L, Hauser KE, Simmerling C. ff14SB: improving the accuracy of protein side chain and backbone parameters from ff99SB. *J Chem Theory Comput*. 2015;11:3696-3713.
65. Izadi S, Anandakrishnan R, Onufriev AV. Building water models: a different approach. *J Phys Chem Lett*. 2014;5:3863-3871.
66. Ryckaert J-P, Ciccotti G, Berendsen HJC. Numerical integration of the Cartesian equations of motion of a system with constraints: molecular dynamics of *n*-alkanes. *J Comput Phys*. 1977;23:327-341.
67. Miyamoto S, Kollman PA. Settle: an analytical version of the SHAKE and RATTLE algorithm for rigid water models. *J Comput Chem*. 1992;13:952-962.
68. Nguyen H, Roe DR, Simmerling C. Improved generalized born solvent model parameters for protein simulations. *J Chem Theory Comput*. 2013;9:2020-2034.
69. Yokoyama T, Mizuguchi M, Nabeshima Y, et al. Hydrogen-bond network and pH sensitivity in transthyretin: neutron crystal structure of human transthyretin. *J Struct Biol*. 2012;177:283-290.
70. Penchala SC, Connelly S, Wang Y, et al. AG10 inhibits amyloidogenesis and cellular toxicity of the familial amyloid cardiomyopathy-associated V122I transthyretin. *Proc Natl Acad Sci U S A*. 2013;110:9992-9997.
71. Park GY, Jamerlan A, Shim KH, An SSA. Diagnostic and treatment approaches involving transthyretin in amyloidogenic diseases. *Int J Mol Sci*. 2019;20:2982.
72. Chiti F, Dobson CM. Protein misfolding, functional amyloid, and human disease. *Annu Rev Biochem*. 2006;75:333-366.
73. Kollmer M, Close W, Funk L, et al. Cryo-EM structure and polymorphism of Aβ amyloid fibrils purified from Alzheimer's brain tissue. *Nat Commun*. 2019;10:4760.

SUPPORTING INFORMATION

Additional supporting information can be found online in the Supporting Information section at the end of this article.

How to cite this article: Hartmann J, Zacharias M. Analysis of amyloidogenic transthyretin mutations using continuum solvent free energy calculations. *Proteins*. 2022;90(12):2080-2090. doi:10.1002/prot.26399